We notice the increased values of the specificity (TN rate) obtained for the first three classifiers (SVM, MLP and RF).

TABLE I. THE CLASSIFICATION PERFORMANCE PARAMETERS OBTAINED IN THE CASE WHEN THE ENTIRE SET OF THE LAWS' FEATURES WAS CONSIDERED, FOR THE DIFFERENTIATION BETWEEN THE COLORECTAL TUMORS AND IBD

| | Rec. Rate | TP Rate | TN Rate | AUC |
|---|---|---|---|---|
| **SVM** | **98.33%** | **96.7%** | **98.5%** | **98.33%** |
| **MLP** | **96.66%** | **93.3%** | **98.33%** | **96.66%** |
| **RF** | **95%** | **93.3%** | **96.7%** | **95%** |
| **AdaBoost + J48** | **93.3%** | **96.7%** | **90%** | **93.3%** |

We also compared the classification accuracies obtained in the case when using only the old textural feature set with those obtained in the case when using the entire set of textural features (including the CTMCM features). As it results from the next figure (Fig. 2), in the case when considering the entire set of Laws' features, the newly resulted recognition rates overpassed the old recognition rates, in all cases.

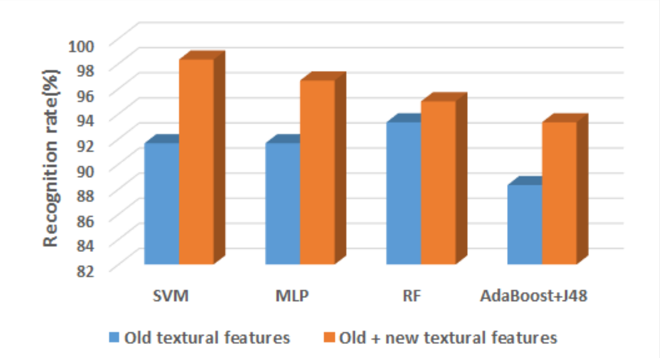


Fig. 2. The comparison between the recognition rates resulted for the old and new textural feature sets, when all the Laws' features were considered, in the case of the differentiation between colorectal tumors and IBD

- *The case when only the selected Laws' features were considered*

The relevant textural features obtained in this case are provided in (4). We notice the presence of the CTMCM based homogeneity, energy and contrast, as well as of the third order CTMCM based correlation and contrast, denoting the heterogeneity and complex structure of the tumoral tissue, respectively differences in granularity between the tumoral tissue and the non-tumoral one (through the third order CTMCM correlation).

{GLCM_variance, Autocorrelation_index, Directional_grad_magnitude, Directional_grad_variance, GLCM5_Entropy, GLCM5_Variance, EOCM3_ Homogeneity, EOCM3_Energy, EOCM3_Entropy, EOCM3_Contrast, EOCM3_Variance, GLCM3_Homogeneity, GLCM3_Entropy, GLCM3_Correlation, ***CTMCM_Homogeneity***, ***CTMCM_Energy***, ***CTMCM_Contrast***, ***CTMCM3_Correlation***, ***CTMCM3_Contrast}*** (4)

The values of the classification performance parameters obtained in this case are depicted in Table II. As it results from Table II, the maximum recognition rate obtained in this situation, of 97.5%, corresponded to the RF classifier, being slightly lower than the maximum accuracy obtained in the previous case. We notice the increased values of the specificity (TN rate) in this case as well.

TABLE II. THE CLASSIFICATION PERFORMANCE PARAMETERS OBTAINED IN THE CASE WHEN THE SELECTED LAWS' FEATURES WERE CONSIDERED, FOR THE DIFFERENTIATION BETWEEN THE COLORECTAL TUMORS AND IBD

| | Recogn. Rate | TP Rate | TN Rate | AUC |
|---|---|---|---|---|
| **SVM** | **97.33%** | **94%** | **98.7%** | **97.3%** |
| **MLP** | **96.66%** | **91.7%** | **98.7%** | **98.1%** |
| **RF** | **97.5%** | **95.3%** | **98.7%** | **99.8%** |
| **AdaBoost + J48** | **91.81%** | **86.3%** | **96.3%** | **97.4%** |

When performning the comparison of the entire set of the textural features (containing both the old and the newly defined features) with the old textural feature set, we noticed an increase in classification accuracy for the first mentioned set, in most of the situations. This result is illustrated in the figure below (Fig. 3).

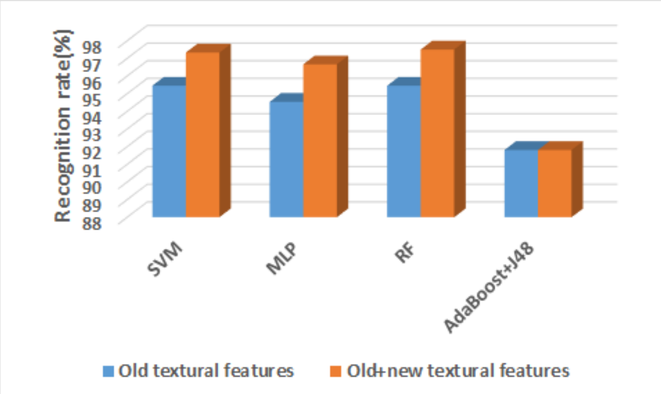


Fig. 3. The comparison between the recognition rates resulted for the old and new textural feature sets, when only the selected Laws' features were considered, in the case of differentiation between colorectal tumors and IBD

2) *The differentiation between the gingival sulcus and the neighboring areas*

- *The case when all the Laws' features were considered*

The set of the relevant textural features for the differentiation between the gingival sulcus and the surrounding areas is provided in (5):

{ GLCM_Energy, Autocorrelation_index, Edge,orientation_variability, Wavelet_Entropy7_lh, Wavelet_Entropy7_hl, Wavelet_Entropy7_hh, Wavelet_Entropy8_hh, Laws_level_mean, Laws_level_frequency, Laws_ripple_mean, Laws_ripple_frequency, ***CTCM_Homogeneity***, ***CTMCM_Entropy***, ***CTMCM_Correlation***, ***CTMCM3_ Homogeneity***, ***CTMCM3_Energy***, ***CTMCM3_Entropy***, ***CTMCM3_Correlation***} } (5)

We notice, in (5), the presence of the second order CTMCM features, as well as of the third order CTMCM features. The homogeneity, energy and entropy, derived from the second and third order CTMCM matrices, stand for the more homogeneous and hypoechogenic nature of the gingival sulcus region, in comparison with the sourrounding areas. The correlation computed from the second, respectively from the third order CTMCM, together with the autocorrelation index, denote differences in granularity between the gingival sulcus and the neighboring regions.

The values of the classification performance parameters, obtained after the selection of the relevant textural features, in the case of separation between the gingival sulcus and the surrounding regions, are provided in Table III. The maximum recognition rate, of 93.05%, the maximum specificity, of 91.7%, as well as the maximum AUC, of 97.4%, resulted in the case of the RF classifier. The maximum specificity, of 94.4%, resulted in both cases of the RF and MLP classifiers.

TABLE III. THE CLASSIFICATION PERFORMANCE PARAMETERS OBTAINED WHEN ALL THE LAWS' FEATURES WERE CONSIDERED, IN THE CASE OF GINGIVAL SULCUS RECOGNITION

| | Recogn. Rate | TP Rate | TN Rate | AUC |
|---|---|---|---|---|
| **SVM** | **86.11%** | **83.3%** | **88.9%** | **94.7%** |
| **MLP** | **91.66%** | **94.4%** | **88.9%** | **92.1%** |
| **RF** | **93.05%** | **94.4%** | **91.7%** | **97.4%** |
| **AdaBoost + J48** | **88.88%** | **88.9%** | **88.9%** | **91.6%** |

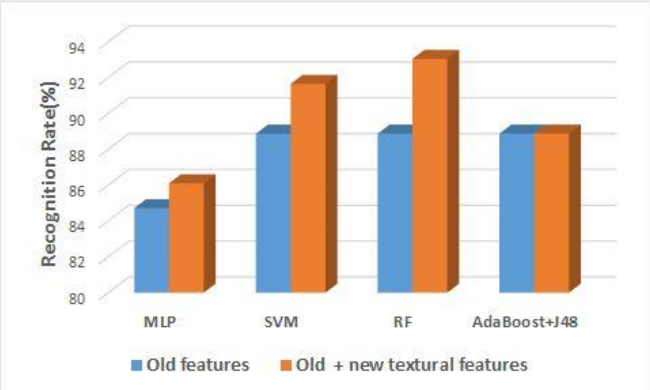


Fig. 4. The comparison between the recognition rates resulted for the old and new textural feature sets, when all the Laws' features were considered, in the case of the differentiation between the gingival sulcus and the surrounding areas

The discrimination power due to the previously existing textural features was compared with that which was due to the set formed by the old textural features and by the newly defined textural features. This comparison is illustrated in the fourth figure. From Fig. 4, we notice that the recognition rate which is due to the newly defined textural features is superior to that provided only by the old textural features in most of the situations, excepting the case of the AdaBoost meta-classifier combined with the J48 basic learner, when the two computed accuracies are equal.

- *The case when only the selected Laws' features were considered.*

The set of the relevant textural features selected in this case is illustrated in (6). We notice the presence of the textural features derived from the CTMCM matrix: the entropy computed from the second and third order CTMCM, respectively the homogeneity computed from the third order CTMCM, stand for the differences in heterogeneity between the structure of the gingival sulcus and the surrounding areas. The contrast derived from the third order CTMCM matrix denote the less complex structure of the gingival sulcus, respectively the more complex structure of the surrounding areas (gum and teeth). We also remark the first order statistics referring to the arithmetic mean and frequency of the simple textural microstructures detected by applying the Laws' convolution filters: levels, edges, spots, waves and ripples.

{ GLCM_Energy, GLCM_Entropy,
Autocorrelation_index,
Edge_orientation_variability,Wavelet_Entropy7_ll,
Wavelet_Entropy8_ll,Wavelet_Entropy8_lh,
Laws_level_mean, Laws_edge_mean, (6)
Laws_spot_mean, Laws_wave_mean,
Laws_ripple_mean, Laws_ripple_frequency,
***CTMCM_Entropy***, ***CTMCM3_Homogeneity***,
***CTMCM3_Entropy***, ***CTMCM3_Contrast***}

The classification performance parameters obtained in this situation, after the selection of the relevant textural features in the case of the differentiation between the gingival sulcus and the neighboring tissues, are illustrated in Table IV.

TABLE IV. THE CLASSIFICATION PERFORMANCE PARAMETERS OBTAINED IN THE CASE WHEN ONLY THE SELECTED LAWS' FEATURES WERE CONSIDERED, IN THE CASE OF GINGIVAL SULCUS RECOGNITION

| | Recogn. Rate | TP Rate | TN Rate | AUC |
|---|---|---|---|---|
| **SVM** | **90.32%** | **91.7%** | **88.9%** | **97%** |
| **MLP** | **90.27%** | **97.2%** | **83.3%** | **88.7%** |
| **RF** | **91.75%** | **97.2%** | **86.1%** | **96.4%** |
| **AdaBoost + J48** | **91.66%** | **94.4%** | **88.9%** | **89%** |

Fig. 5 illustrates the comparison between the recognition rates obtained when considering only the old textural feature set, respectively the set formed by the old and new textural features. As it results from Fig.5, there is always an increase in accuracy for the feature set that includes the newly defined textural features. The best accuracy, of 91.75%, resulted in the case of the RF classifier, being smaller than the maximum accuracy (93.05%) resulted in the case when all the Laws' features were considered in order to define the CTMCM matrix The highest sensitivity, of 97.2% resulted in both cases of MLP and RF classifiers, the highest specificity, of 88.9% resulted in the cases of the SVM classifier, respectively of the combination between the AdaBoost meta-classifier and the J48 learner, while the highest recognition rate, of 97%, resulted in the case of the SVM classifier. We notice that all the values for the recognition rate were above 90% in this situation.

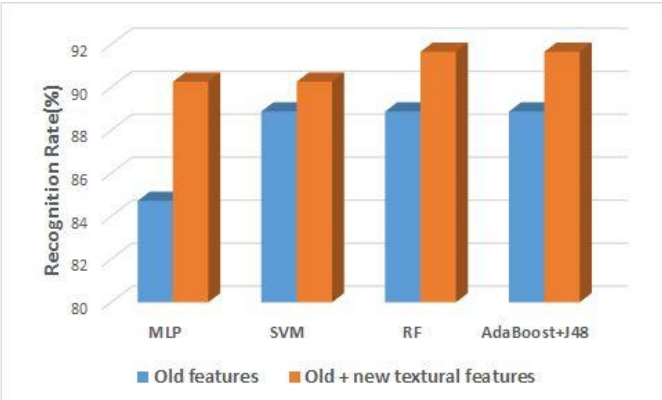


Fig. 5. The comparison between the recognition rates resulted for the old and new textural feature sets, when the selected Laws' features were considered, in the case of the differentiation between the gingival sulcus and the surrounding areas

### *B. The role of the multiresolution CTMCM (MCTMCM) in the recognition of the pathlological structures*

#### *1) Colorectal tumors/IBD differentiation*

The set of the relevant textural features obtained in this case is illustrated in (7). We can remark that also the third order MCTMCM based features: variance, contrast and correlation are included in this set. These features characterize the heterogeneity and the complex grey level structure of the malignant tumors. We can also notice that the relevant MCTMCM features resulted at both resolution levels: at the first level, on the component obtained by applying the combination of the low-pass filters and at the second level, on most of the components.

{Wavelet_Entropy2, Wavelet_Entropy6_ll, Dir_grad_variability, GLCM5_ Entropy, EOCM3_ Coreelation, GLCM3_Energy, ***MCTMCM3 _Variance2, MCTMCM3_ Contrast3_ll, MCTMCM3_Correlation2 _ll, MCTMCM3_ Homogeneity3_lh, MCTMCM3_ Contrast3_hl, MCT MCM3_Homogeneity4_ hh***} (7)

TABLE V. THE CLASSIFICATION PERFORMANCE PARAMETERS OBTAINED IN THE CASE WHEN THE MCTMCM FEATURES WERE CONSIDERED, WHEN DIFFERENTIATING BETWEEN COLORECTAL TUMORS AND IBD

| | Recogn. Rate | TP Rate | TN Rate | AUC |
|---|---|---|---|---|
| **SVM** | **96.36%** | **96.4%** | **96.4%** | **96.4%** |
| **MLP** | **95.45%** | **94.5%** | **96.4%** | **99.4%** |
| **RF** | **95.45%** | **92.7%** | **98.2%** | **98.8%** |
| **AdaBoost + J48** | **93.63%** | **94.5%** | **92.7%** | **94.1%** |

Concerning the classification performance resulted for the relevant feature set depicted in (7), the maximum recognition rate, of 96.36%, was obtained in the case of the SVM classifier, as it results from Table V. We can also notice the increased values of the specificity obtained in this case, as well as the high AUC.

At the end, we compared the classification accuracies obtained for two datasets: for the dataset containing only the old textural features, respectively for that containing both the old and new textural features. The improvement due to the entire feature set is obvious for three classifiers, while for the RF classifier, only a slight improvement was noticed, as it results from the next figure (Fig. 6).

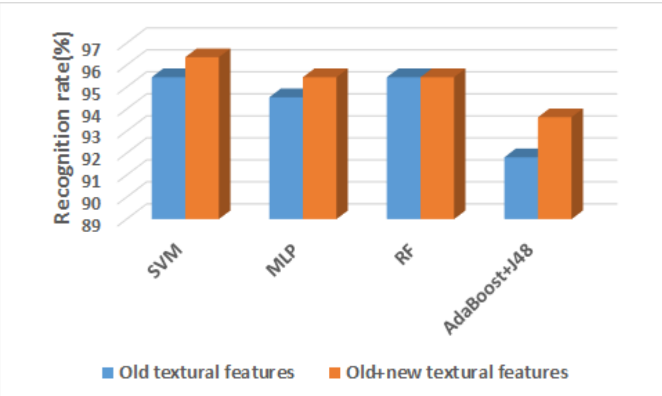


Fig. 6. The comparison between the recognition rates resulted for the old and new textural feature sets, when the MCTMCM features were considered, in the case of the Colorectal tumors/IBD differentiation

#### *2) The differentiation between the gingival sulcus and the neighboring areas*

The set of the relevant textural features for the differentiation between the gingival sulcus and the surrounding tissues, obtained when taking into account the multiresolution third order CTMCM attributes, is illustrated in (8). We notice that, in (8), there are multiple features derived from the MCTMCM matrix of order three. Thus, we remark the presence of the third order MCTMCM homogeneity, corresponding to most of the components on all the considered resolution levels, as well as of the third order MCTMCM entropy and energy, denoting the more heterogeneous structure of the tissues that surround the gingival sulcus; of the third order MCTMCM correlation, denoting differences in granularity, at multiple resolutions, between, the considered classes of tissues, of the third order MCTMCM contrast and variance, denoting the more increased structural complexity of the tissue classes that surround the gingival sulcus.

{GLCM_Energy, GLCM_Contrast, Wavelet_Entropy7_ll, Wavelet_Entropy7_hh Wavelet_Entropy8_hh, ***MCTMCM3_Correlation3, MCTMCM3_Variance4, MCTMCM3_Contrast2_ll, MCTMCM3_Homogeneity4_ll, MCTMCM3_ Energy1_lh, MCTMCM3_ Contrast3_lh, MCTMCM3_Variance2_lh, MCTMCM3_ Entropy2_hl, MCTMCM3_ Contrast1_hl, MCTMCM3_Contrast4_hl, MCTMCM3_Homo geneity2_hl, MCTMCM3_ Homogeneity3_hl, MCTMCM3_Homogeneity2_hh, MCTMCM3_ Homogeneity3_hh, MCTMCM3_Homogeneity4_hh*** } (8)

In Table VI, the values of the classification performance parameters, obtained when providing the set of the relevant textural features illustrated in (8), at the inputs of the considered classifiers, are depicted. The maximum recognition rate, of 92.85%, as well as the maximum AUC, of 96.5%, resulted in the case of the RF classifier. We also notice the increased value of the sensitivity (96.4%), obtained in the case of the MLP classifier.

TABLE VI. THE CLASSIFICATION PERFORMANCE PARAMETERS OBTAINED IN THE CASE WHEN THE MCTMCM FEATURES WERE CONSIDERED, WHEN DIFFERENTIATING BETWEEN THE GINGIVAL SULCUS AND THE NEIGHBORING AREAS

| | Recogn. Rate | TP Rate | TN Rate | AUC |
|---|---|---|---|---|
| **SVM** | **90.28%** | **90.3%** | **90.3%** | **90.3%** |
| **MLP** | **91.07%** | **96.4%** | **85.7%** | **91.1%** |
| **RF** | **92.85%** | **92.9%** | **92.9%** | **96.5%** |
| **AdaBoost + J48** | **90.28%** | **85.7%** | **92.9%** | **91.7%** |

The comparison between the classification accuracies resulted when considering only the old textural features, respectively when taking into account both the old and the newly defined textural features is illustrated in Fig.7. An accuracy increase for all the classifiers, corresponding to the case when also the newly defined textural features were taken into account, can be noticed in this figure.

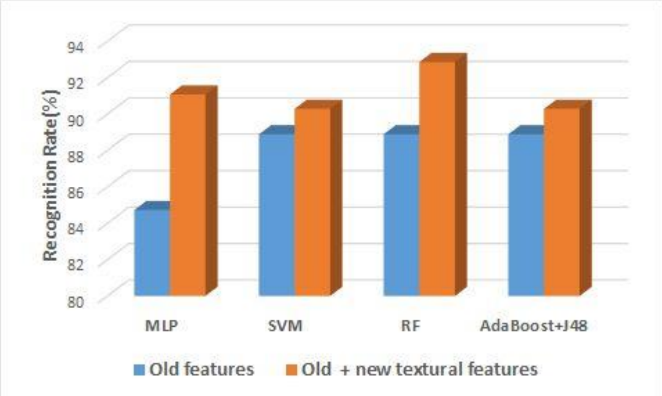


Fig.7. The comparison between the recognition rates resulted for the old and new textural feature sets, when the MCTMCM features were considered, in the case of the differentiation between the gingival sulcus and the surrounding tissues

## V. Conclusions

The Complex Textural Microstructure Co-occurrence Matrix (CTMCM) generally led, in the case of the considered pathological structures, to a classification performance improvement, compared with the situation when using only the old textural features. The best results were obtained when all the Laws' features were considered, but satisfying results were provided also when taking into account the CTMCM matrix based only on the selected Laws' features, respectively the third order MCTMCM based features, especially in the case of the gingival sulcus characterization and recognition. The best obtained classification accuracy was 98.33% in the case of the recognition of the colo-rectal tumors and 93.05% in the case of the gingival sulcus recognition. Thus, in the first case, the result was better than the already obtained results in the domain, while in the second case the result was comparable with the state of the art results.

More extended datasets will be considered in our future work, in order to further validate the CTMCM and MCTMCM methods. Other types of multiresolution textural features will be considered as well, such as those based on the Gabor transform [4].

## References

[1] D. Martínez-Ares, I. Martín-Granizo Barrenechea, J. Souto-Ruzo, J. Yáñez López, A. Pallarés Peral and J. L. Vázquez-Iglesias, "The value of abdominal ultrasound in the diagnosis of colon cancer", *Revista Espanola des Enfermedades Digestiva*, vol. 97, no.12, pp.877-886, 2005.

[2] L. Ruess "Inflammatory bowel disease in children and young adults: correlation of sonographic and clinical parameters during treatment", *American Journal of Roentgenology*, vol.175, no.1, pp.79-84, 2000.

[3] A. Nanci, D. Bosshardt, "Structure of periodontal tissues in health and disease", *Periodontology 2000*, vol.40, no.1, pp. 11–28, 2006.

[4] A. Meyer-Base, *Pattern recognition for medical imaging*, Elsevier, 2009.

[5] H.Sujana, S.Swarnamani, "Application of Artificial Neural Networks for the classification of liver lesions by texture parameters", *Ultrasound in Medicine & Bio*logy, vol. 22, no. 9, pp. 1177 –1181, 1996.

[6] T.Chikui, "Sonographic texture characterization of salivary gland tumors by fractal analysis", *Ultrasound in Medicine & Biology*, vol. 31, no. 10, pp.1297- 1304, 2005.

[7] H.Yoshida, D.Casalino, "Wavelet packet based texture analysis for diferentiation between benign and malignant liver tumors in ultrasound images*", Physics in Medicine & Biology*, vol. 48, pp. 3735-3753, 2003.

[8] A.Madabhushi, "Automated Detection of Prostatic Adenocarcinoma from High-Resolution Ex Vivo MRI", *IEEE Transactions on Medical Imaging*, pp.1611-1626, 2005.

[9] K. Masood, "Co-occurrence and morphological analysis for colon tissue biopsy classification", *Proceedings of the 4th International Workshop on Information Technology*, Pakistan, pp. 211-216, 2006.

[10] D. Mitrea, P. Mitrea, S. Nedevschi, R. Badea, "Abdominal tumor characterization and recognition using superior order cooccurrence matrices, based on ultrasound images", *Computational and Mathematical Methods in Medicine*, 17 pages, 2012.

[11] D. Mitrea, S. Nedevschi, M. Socaciu, R. Badea, "The Role of the Superior Order GLCM in the Characterization and Recognition of the Liver Tumors from Ultrasound Images", *Radioengineering*, vol. 21, no. 1, pp. 79-85, 2012.

[12] B. Sujatha, V. Kumar, P. Harini, "A new logical compact LBP Co-Occurrence Matrix for Texture Analysis", *International Journal of Scientific & Engineering Research*, vol. 3, no. 2, pp. 1-5, 2012.

[13] B. Sujatha, C. Sekhar Reddi, "Texture classification using texton co-occurrence matrix derived from texture orientation", *International Journal on Soft Computing and Engineering*, vol. 2, no. 6, pp. 18-23, 2013.

[14] D. Mitrea, S. Nedevschi, R. Badea, "The Role of the Textural Microstructure Coocurrence Matrices in the Classification of the Abdominal Tumors", *10th IEEE ICCP 2014 Conference*, T.U.Cluj-Napoca, pp. 187-190, 2014.

[15] K. I. Laws, „Rapid texture identification", *SPIE Vol. 238, Image Processing for Missile Guidance*, pp.76-380, 1980.

[16] M. Hall, "Benchmarking attribute selection techniques for discrete class data mining", *IEEE Transactions On Knowledge and Data Engineering*, vol. 15, no. 3, pp. 1-16, 2003.

[17] Weka3, Data Mining Software in Java, 2014, Online: http://www.cs.waikato.ac.nz/ml/weka.

[18] R. Duda, *Pattern Classification*, Wiley Interscience, 2003.